High-Field Energy Distribution, Mobility, and Diffusion of Heavy Holes in p-Germanium

G. Persky and D. J. Bartelink

Bell Telephone Laboratories, Murray Hill, New Jersey 07974

(Received 5 September 1969)

A novel approximation scheme for hot-carrier distribution functions is introduced and employed in a calculation of the high-field mobility and diffusion coefficients of heavy holes in p-Ge at 77°K. It is assumed that the heavy-hole band has an isotropic and momentum-independent effective mass, and that the holes are scattered elastically by acoustic phonons and inelastically by optical phonons. Interaction with the light-hole and split-off bands is neglected. The principal results of the calculation are as follows: Over the decade 1 kV/cm $<E<$ 10 kV/cm the mobility obeys the power-law relation $\mu \propto E^{-0.8}$. The diffusion tensor is moderately anisotropic with $D_{||}>D_{\perp}$, but neither coefficient departs greatly from the zero-field diffusion constant, 250 cm²/sec, in the field range up to 35 kV/cm. The calculation method makes use of a parametrized model of the distribution function which characterizes the energy dependence of its angular average by two distinct Maxwellians intersecting at the optical-phonon energy, but which makes no *a priori* assumptions about the angular dependence of the distribution function. Solution for the Maxwellian temperatures is effected by means of a special set of "anisotropy balance equations." These equations involve only the isotropic part of the distribution function and may be used to obtain the parameter values of any parametrized energy distribution, of which the present model is but a special case. Following a procedure originally outlined by Wannier, a derivation of these equations is given first for isotropic scattering and a spherical, constant mass, as required for the p-Ge calculation. An alternative method is used to derive a more general set of balance equations valid for scattering probabilities of the form $P(|\mathbf{k}-\mathbf{k'}|)$ and spherical bands of arbitrary dispersion law. An error-estimate criterion is formulated. This criterion permits evaluation of the influence on calculated transport quantities of distribution-function parametrizations with one additional parameter.

I. INTRODUCTION

IN this paper the high-field distribution function and transport properties of p-Ge are investigated theoretically with an aim toward determining the high-field bulk diffusion tensor.[1] Although some theoretical studies of diffusion in barrier and junction regions have been carried out,[2] high-field diffusion in bulk semiconductors is of interest in its own right. Gunn domains[3] and avalanche transit time instabilities[4] are influenced by it. The possibility of diffusion-induced instabilities has been advanced by several authors.[5] Measurement of the field dependence and anisotropy of the diffusion tensor might also provide another experimental handle on the form of hot-carrier distribution functions. Unfortunately, the experimental picture at this time is somewhat incomplete. An investigation of transverse noise temperature in n-Ge has been carried out by Erlbach and Gunn.[6] Okamoto *et al.*[7] employed a variation of the Haynes-Shockley technique to measure the longitudinal diffusion of minority holes injected into n-Ge under high-field conditions. The possibility of considerable overestimation of the hole diffusion coefficient appears inherent in their experiment. Indeed, the values they obtained are considerably higher than what might be reasonably inferred from the work of Erlbach and Gunn.

In view of the current paucity of experimental data, a model calculation of the high-field diffusion which does not simply assume an Einstein relation would appear to be justified. Ours is undertaken in this spirit and several complications peculiar to p-Ge are accordingly avoided. We treat the heavy-hole band as spherical parabolic and disregard interaction with the light-hole and split-off bands. Errors associated with neglect of the light-hole band should not be large because of its low density of states, while inaccuracies due to neglect of the split-off band are anticipated only at extremely high fields; the results should therefore be reliable over most of the field range considered (470 V/cm $<E<$ 36 000 V/cm). Qualitatively similar behavior might be expected in n-Ge and n-Si, at least when the electric field is applied in a direction of equal valley heating.

With the above simplifications the major problem remains that of finding, over the field range of interest, the distribution function of heavy holes accelerated by the field and scattered by optical and acoustic phonons. There is experimental[8] and theoretical evidence[9-11] that when the lattice temperature is 77°K, at least over the lower-field portion of the hot-carrier regime this distribution function is composed of two Maxwellians intersecting near the optical-phonon energy. One would think that such prior knowledge of the energy depen-

[1] A preliminary report on this work has already been given. See G. Persky and D. J. Bartelink, Phys. Letters **28A**, 749 (1969).

[2] R. Stratton, Phys. Rev. **126**, 2002 (1962); R. Stratton and E. I. Jones, J. Appl. Phys. **38**, 4596 (1967).

[3] J. B. Gunn, Solid State Commun. **1**, 88 (1963).

[4] W. T. Read, Jr., Bell System Tech. J. **37**, 401 (1958); T. Misawa, IEEE Trans. Electron Device **ED-13**, 137 (1966); **ED-13**, 143 (1966).

[5] W. P. Dumke, Appl. Phys. Letters **10**, 314 (1967); K. Blötekjaer and P. Weissglas, J. Appl. Phys. **39**, 1645 (1968).

[6] E. Erlbach and J. B. Gunn, Phys. Rev. Letters **8**, 280 (1962).

[7] K. Okamoto, J. Nishizawa, and K. Takahashi, J. Appl. Phys. **36**, 3716 (1965).

[8] A. C. Baynham and E. G. S. Paige, Phys. Letters **6**, 7 (1963).

[9] T. Kurosawa, J. Phys. Soc. Japan **21**, 424 (1966).

[10] H. F. Budd, J. Phys. Soc. Japan **21**, 420 (1966).

[11] H. Budd, Phys. Rev. **158**, 798 (1967).

dence, judiciously employed in conjunction with a suitable approximation scheme, should facilitate a sufficiently accurate calculatron of the distribution function with more insight and far less exhaustive computations than is inherent in those available techniques that are, in principle, exact.[9–12] The well-known ways of obtaining approximate solutions to the Boltzmann equation, however, do not permit ready utilization of information solely about the energy distribution. Angular truncations[13,14] of this equation build into the distribution function one or another set of restrictions on its angular form. Moment balance techniques[15] have invariably been applied to the drifted Maxwellian approximation,[16] in which is implicit a different, but equally severe, set of energy-angle constraints. We have therefore found it advantageous to employ a method that permits us to make all *a priori* assumptions about the *energy* dependence of the distribution function, while requiring no explicit approximations in the *angular* dependence.

The method makes use of moment balance equations, which we call "anisotropy balance equations," that incorporate the kinetic content of the Boltzmann equation and involve only the isotropic part of the distribution function. There are several ways in which such equations can be generated from the Boltzmann equation; a direct procedure was outlined in a lengthy article on gaseous plasmas by Wannier,[17] but there has been apparently no previous application to semiconductor physics. Section II is therefore devoted to a derivation, paralleling that of Wannier, for the case of isotropic scattering of carriers in a spherical parabolic band. An alternative derivation, valid for nonparabolic bands and more arbitrary scattering laws, and an error-analysis technique which extends the power of the method, are developed in the Appendices. In Sec. III a two-Maxwellian parametrized model of the heavy-hole distribution is introduced, and the parameter values determined by means of the balance equations. The results of our mobility and diffusion coefficient calculations are presented in Secs. IV and V, and compared therein with the available experimental data.

II. ANISOTROPY BALANCE EQUATIONS

Consider an unobunded homogeneous slab of semiconductor in which one species of carriers predominates, and to which is applied a uniform time-independent electric field. If the density of carriers is low enough to allow neglect of carrier-carrier interaction, then the motion of the carriers is governed by the steady-state Boltzmann equation

$$\mathbf{F} \cdot \nabla_p f(\mathbf{p}) = \int f(\mathbf{p}')S(\mathbf{p}',\mathbf{p})d^3p' - \nu(\mathbf{p})f(\mathbf{p}), \quad (1)$$

where $\mathbf{F}$ is the field force $q\mathbf{E}$, $\mathbf{p}$ is the crystal momentum, $f(\mathbf{p})$ is the distribution function of the carriers in momentum space, $S(\mathbf{p}',\mathbf{p})$ is the probability per unit time of a carrier being scattered from $\mathbf{p}'$ to $\mathbf{p}$, and $\nu(\mathbf{p}) = \int S(\mathbf{p},\mathbf{p}')d^3p'$ is the collision frequency.

We are interested in the distribution function for heavy holes in a spherical parabolic band characterized by an effective mass m, and for which the scattering is by nonpolar optical phonons and by acoustic phonons at temperatures high enough for equipartition[18] to apply. Under these conditions (a) the collison frequency is a function solely of the energy $\epsilon = p^2/2m$, (b) the scattering is isotropic, and (c) the solution to (1) has rotational symmetry about the axis in p-space parallel to the field, and hence may be expanded in a series of Legendre polynomials with coefficients dependent on the energy alone, i.e.,

$$f(\mathbf{p}) = \sum_{l=0}^{\infty} n_l(\epsilon)P_l(\cos\theta), \quad (2)$$

where θ is the angle that $\mathbf{p}$ makes with the field. When (2) is substituted into (1), the entire equation may be expanded in Legendre polynomials. Upon separately nulling the coefficient of each polynomial, there then results the well-known infinite Boltzmann hierarchy of coupled differential equations.[19] For isotropic scattering only $n_0(\epsilon)$, the isotropic part of the distribution funcion, contributes to the integral on the right-hand side of (1), and these coupled equations take the form

$$\tfrac{1}{3}F(d/d\epsilon)(\epsilon n_1) = (\tfrac{1}{2}m)^{1/2}\epsilon^{1/2}\hat{S}n_0,$$

$$F[\tfrac{2}{5}(d/d\epsilon)(\epsilon^{3/2}n_2) + \epsilon^{3/2}(dn_0/d\epsilon)] = -(\tfrac{1}{2}m)^{1/2}\epsilon\nu n_1,$$

$$\vdots \qquad\qquad \vdots \qquad (3)$$

$$F\left(\frac{(l+1)}{(2l+3)}\frac{d}{d\epsilon}(\epsilon^{1+\frac{1}{2}l}n_{l+1}) + \frac{l}{2l-1}\epsilon^{l+\frac{1}{2}}\frac{d}{d\epsilon}(\epsilon^{\frac{1}{2}-\frac{1}{2}l}n_{l-1})\right)$$

$$= -(\tfrac{1}{2}m)^{1/2}\epsilon^{\frac{1}{2}+\frac{1}{2}l}\nu n_l.$$

In the first member of (3), $\hat{S}$ is a scattering operator defined by

$$\hat{S}n_0(\epsilon) = \int n_0(\epsilon')S(\mathbf{p}',\mathbf{p})d^3p' - \nu n_0(\epsilon). \quad (4)$$

To generate the required set of anisotropy balance equations the following approach[17] is most direct. Each equation in (3) has been written such that its highest-order term appears only in a total derivative with respect to energy. Hence an energy integration from zero

[12] H. D. Rees, Phys. Letters **26A**, 416 (1968).
[13] P. A. Wolff, Phys. Rev. **95**, 1415 (1954).
[14] G. A. Baraff, Phys. Rev. **133**, A26 (1964).
[15] R. Stratton, Proc. Roy. Soc. (London) **A242**, 355 (1957).

[16] P. P. Debye and E. M. Conwell, Phys. Rev. **93**, 693 (1954).
[17] G. H. Wannier, Bell System Tech. J. **32**, 170 (1953), p. 218.
[18] E. M. Conwell, *High Field Transport in Semiconductors* (Academic Press Inc., New York, 1967), p. 7.
[19] Reference 17, p. 197.

to infinity of the general member of the hierarchy yields

$$F\frac{(l+1)}{(2l+3)}(\epsilon^{1+\frac{1}{2}l}n_{l+1})\Big|_0^\infty + \frac{l}{2l-1}\int_0^\infty \epsilon^{l+\frac{1}{2}}\frac{d}{d\epsilon}(\epsilon^{\frac{1}{2}-\frac{1}{2}l}n_{l-1})d\epsilon$$

$$= -(\tfrac{1}{2}m)^{1/2}\int_0^\infty \epsilon^{\frac{3}{2}+\frac{1}{2}l}\nu n_l d\epsilon. \quad (5)$$

At high enough energies all n_l should fall off exponentially and thus faster than any power of ϵ. At $\epsilon=0$ it is reasonable to expect n_l to be nonsingular, or at worst only weakly singular, so that $\epsilon^{1+\frac{1}{2}l}n_{l+1}=0$. Therefore, the first term on the left in (5) should vanish. Similar considerations allow a partial integration to be performed on the second term on the left. The result for $l=0$ is

$$0 = (\tfrac{1}{2}m)^{1/2}\int_0^\infty \epsilon^{1/2}\hat{S}n_0 d\epsilon, \quad (6a)$$

while for $l\geq 1$,

$$\frac{l(2l+1)}{2(2l-1)}F\int_0^\infty \epsilon^{\frac{1}{2}l}n_{l-1}d\epsilon = (\tfrac{1}{2}m)^{1/2}\int_0^\infty \epsilon^{\frac{3}{2}+\frac{1}{2}l}\nu n_l d\epsilon. \quad (6b)$$

Clearly, the integration process breaks the infinite chain of the Boltzmann hierarchy (3); when carried out on the lth member of (3) it produces a relation in which the $(l+1)$th term in that member is absent.

Equation (6a) may be immediately recognized as the continuity equation, which is satisfied identically for any physical scattering mechanism independently of n_0. In Appendix A it is shown that the $l=1$ and $l=2$ members of (6b) are, respectively, momentum and power balance relations. Larger values of l lead to analogous moment equations of higher order. By means of algebraic substitutions and manipulations involving the lower-order members of the hierarchy (3), each of these equations may be reduced to a distinct integral relation involving only $n_0(\epsilon)$, the energy distribution. The derivation for $l=1$ is carried out below. For higher l values the procedure is essentially the same but requires considerably more algebra. Therefore, only the results will be given for $l=2$ and $l=3$.

With $l=1$, Eq. (6b) becomes

$$\tfrac{3}{2}F\int_0^\infty \epsilon^{1/2}n_0 d\epsilon = (\tfrac{1}{2}m)^{1/2}\int_0^\infty \epsilon\nu n_1 d\epsilon. \quad (7)$$

Let us define η to be the indefinite energy integral of the collision frequency:

$$\eta \equiv \int_0^\epsilon \nu d\epsilon. \quad (8)$$

The function η is introduced into (7) by carrying out

a partial integration of the right-hand side:

$$\tfrac{3}{2}F\int_0^\infty \epsilon^{1/2}n_0 d\epsilon = -(\tfrac{1}{2}m)^{1/2}\int_0^\infty \eta\frac{d}{d\epsilon}(\epsilon n_1)d\epsilon. \quad (9)$$

We eliminate n_1 by substituting the $l=0$ member of (3) into (9). Hence,

$$\frac{F^2}{m}\int_0^\infty \epsilon^{1/2}n_0 d\epsilon + \int_0^\infty \epsilon^{1/2}\eta\hat{S}n_0 d\epsilon = 0. \quad (10a)$$

Equation (10a) is the first member of the set of balance relations for n_0, (6a) constituting the zeroth member. Subsequent equations in this infinite set are generated by starting from higher l values in (6b). For $l=2$ and $l=3$ one obtains, respectively,

$$\frac{F^2}{m}\left(\int_0^\infty \epsilon^{3/2}(\hat{S}-\tfrac{1}{2}\nu)n_0 d\epsilon - \tfrac{3}{4}\int_0^\infty \epsilon^{1/2}\eta n_0 d\epsilon\right)$$

$$- \tfrac{3}{8}\int_0^\infty \epsilon^{1/2}\eta^2\hat{S}n_0 d\epsilon = 0, \quad (10b)$$

$$9\frac{F^4}{m^2}\int_0^\infty \epsilon^{3/2}n_0 d\epsilon$$

$$+ \frac{F^2}{m}\left(7\int_0^\infty \epsilon^{3/2}\eta\hat{S}n_0 d\epsilon - 3\int_0^\infty \epsilon^{1/2}\xi\hat{S}n_0 d\epsilon\right.$$

$$\left. - 4\int_0^\infty \epsilon^{3/2}\eta\nu n_0 d\epsilon - \tfrac{3}{2}\int_0^\infty \epsilon^{1/2}\eta^2 n_0 d\epsilon\right)$$

$$- \tfrac{1}{2}\int_0^\infty \epsilon^{1/2}\eta^3\hat{S}n_0 d\epsilon = 0. \quad (10c)$$

In (10c) the function ξ is a double integral of the collision frequency and may be defined by

$$\xi \equiv \int_0^\epsilon \eta d\epsilon. \quad (11)$$

Whereas the equations in (6b) are simply moment balance relations, those in (10) also incorporate the kinetic content of the Boltzmann equation and therefore increase rapidly in complexity with increasing order. Because the new equations contain only the isotropic part of the distribution function, symmetry requires that they be even functions of the field. Equations (10a) and (10b) are quadratic in F; (10c) is quartic. The $l=4$ equation would also be quartic. In general, one may verify that the lth equation will contain F^{l+1}, F^{l-1}, ..., F^0 for l odd, and F^l, F^{l-2}, ..., F^0 for l even. It seems appropriate to refer to the members of (10) as anisotropy balance equations for the following reason. Given an energy distribution n_0, which may or may not be exact, the Boltzmann hierarchy (3) can be used to generate

the remainder of the distribution function in the form of indefinite energy integrals of n_0 and $\hat{S}n_0$. In demanding that n_0 satisfy the lth member of (10), one guarantees that the anisotropic components n_{l-1} and n_l of this distribution function satisfy the lth moment balance relation in (6); the angular dependence of the distribution function is thereby automatically adjusted. The isotropic part of the exact distribution function must satisfy all members of the infinite set (10).

A generalization of these equations to nonparabolic bands and anisotropic scattering is given in Appendix B.

To use the anisotropy balance equations in an approximation scheme one chooses, on physical grounds or on the basis of prior knowledge, a suitably parametrized form for the energy distribution. The parameter values are then determined by simultaneous solution of as many anisotropy balance equations as there are parameters. Starting with (10a), the equations should be selected sequentially to satisfy the lowest-order moment relations first and thereby ensure a progressive resolution of the angular details of the distribution function. A two-parameter distribution function fitted to (10a) and (10b) satisfies the important momentum and power balance relations and is therefore capable of yielding reasonable accuracy in the calculation of transport quantities which depend only on these few moments of $f(\mathbf{p})$.

The final form (linear, transcendental, piecewise, etc.) of the anisotropy balance equations will depend upon the particular way in which the energy distribution is parametrized. Therefore, the existence and uniqueness of solutions cannot be proven in general, although these properties can be established in certain cases—linear parametrizations, for example. Assuming the existence of unique solutions for a chosen parametrized distribution, it is also desirable to have a measure of the confidence with which transport quantities can be predicted from it. An error-analysis technique that permits one to estimate the change in calculated transport quantities that would be brought about by the introduction of an additional parameter into an m-parameter energy distribution is developed in Appendix C.

III. TWO-TEMPERATURE ENERGY DISTRIBUTION

It has been observed experimentally[8] that at a lattice temperature of 77° and an applied field of 1000 V/cm, the energy distribution of the heavy holes in p-Ge corresponds very closely to two Maxwellians intersecting near the optical-phonon energy ϵ_0. The Maxwellian temperature of the holes above ϵ_0 was found to be lower than that of those below. Detailed calculations[9-11] carried out subsequent to this experiment indicate that, at least for fields in the lower portion of the hot-carrier regime ($E < 2000$ V/cm), scattering of the holes by the optical and acoustic phonons can indeed give rise to an energy distribution of this form. On the other hand, in the extreme high-field limit the same scattering mechanisms are known to lead to the saturated drift velocity regime in which the distribution function becomes a nearly isotropic single Maxwellian.[20] Therefore, a "two-temperature model" of the distribution function, in which the energy dependence is characterized a priori by two Maxwellians intersecting near ϵ_0, ought to provide an accurate representation in both limiting ranges of field strengths; for intermediate fields it remains at least a reasonable interpolation. In this paper we adopt such a model at the outset, for convenience placing the intersection point exactly at the optical-phonon energy. We suppose that n_0 is given by

$$n_0(\epsilon) = N e^{-\epsilon_0/kT_\beta} e^{(\epsilon_0-\epsilon)/kT_\alpha} \quad (\epsilon < \epsilon_0)$$
$$= N e^{-\epsilon/kT_\beta} \quad (\epsilon > \epsilon_0), \tag{12}$$

where N is the normalization, k is the Boltzmann constant, and T_α and T_β are, respectively, the hole temperatures below and above the optical-phonon threshold.

The values of T_α and T_β are determined with the anisotropy balance equations (10a) and (10b). For optical-phonon and elastic acoustic scattering, evaluation of the collision integrals defining ν and $\hat{S}n_0$ is straightforward.[11] At 77°K, in the presence of electric fields sufficiently high to produce a large departure of the distribution function from thermal equilibrium, it is permissible to neglect the absorption of optical phonons and we obtain

$$\nu(\epsilon) = (2/m)^{1/2} [(1/l_0)(\epsilon-\epsilon_0)^{1/2} + (1/l_a)\epsilon^{1/2}], \tag{13}$$

$$\hat{S}n_0(\epsilon) = \frac{(2/m)^{1/2}}{l_0} [(\epsilon+\epsilon_0)^{1/2}n_0(\epsilon+\epsilon_0)$$
$$- (\epsilon-\epsilon_0)^{1/2}n_0(\epsilon)]. \tag{14}$$

In accordance with (8), an energy integration of (13) yields η:

$$\eta(\epsilon) = \tfrac{2}{3}(2/m)^{1/2}[(1/l_0)(\epsilon-\epsilon_0)^{3/2} + (1/l_a)\epsilon^{3/2}]. \tag{15}$$

In (13)–(15), l_a is the constant mean free path for elastic acoustic scattering and l_0 is the high-energy limiting value of the mean free path for optical-phonon scattering. The various powers of $(\epsilon-\epsilon_0)^{1/2}$ are replaced by zero for $\epsilon < \epsilon_0$. Upon inserting (12)–(15) into (10a) and (10b), and making appropriate changes of variables, there results the following pair of coupled transcendental equations for T_α and T_β:

$$(Q\epsilon_0)^2 \int_0^\infty (\epsilon+\epsilon_0)^{1/2} e^{-\epsilon/kT_\beta} d\epsilon + \int_0^{\epsilon_0} \epsilon^{1/2} e^{(\epsilon_0-\epsilon)/kT_\alpha} d\epsilon$$

$$+ \tfrac{4}{3} \int_0^\infty (\epsilon+\epsilon_0)^{1/2} [\epsilon^{3/2} + \rho(\epsilon+\epsilon_0)^{3/2}]$$

$$\times [e^{-\epsilon_0/kT_\beta}(\epsilon+2\epsilon_0)^{1/2} - \epsilon^{1/2}] e^{-\epsilon/kT_\beta} d\epsilon = 0, \tag{16}$$
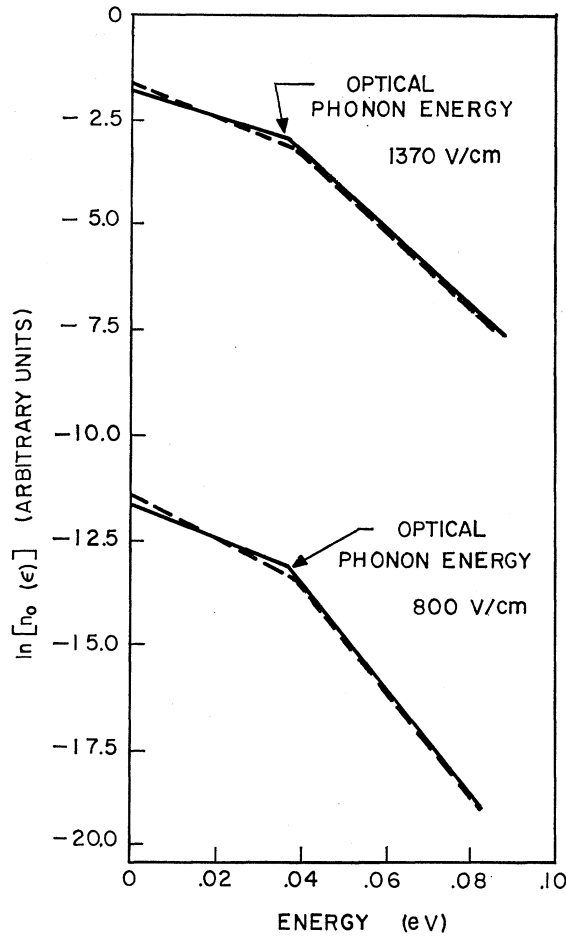
---

[20] Reference 18, Sec. IV. 3.

FIG. 1. Energy distributions at $E=800$ and 1370 V/cm. The solid curves are the two-temperature-model results. The dashed curves are the energy distributions calculated by Budd (Refs. 11 and 12).

$$(Q\epsilon_0)^2 \Bigg(\int_0^\infty \Big[e^{-\epsilon_0/kT\beta}(\epsilon+2\epsilon_0)^{1/2}(\epsilon+\epsilon_0)^{3/2}$$

$$-\tfrac{3}{2}\epsilon^{1/2}(\epsilon+\epsilon_0)^{3/2}-\tfrac{1}{2}\epsilon^{3/2}(\epsilon+\epsilon_0)^{1/2}-\rho(\epsilon+\epsilon_0)^2 \Big] e^{-\epsilon/kT\beta}d\epsilon$$

$$-\rho \int_0^{\epsilon_0} \epsilon^2 e^{(\epsilon_0-\epsilon)/kT\alpha}d\epsilon \Bigg)$$

$$-\tfrac{1}{3}\int_0^\infty \Big[e^{-\epsilon_0/kT\beta}(\epsilon+2\epsilon_0)^{1/2}-\epsilon^{1/2} \Big]$$

$$\times\Big[\epsilon^{3/2}+\rho(\epsilon+\epsilon_0)^{3/2}\Big]e^{-\epsilon/kT\beta}d\epsilon=0. \quad (17)$$

Here Q and ρ are dimensionless quantities defined by

$$Q=Fl_0/\epsilon_0, \quad (18)$$

$$\rho=l_0/l_a. \quad (19)$$

They are, respectively, the ratio of the energy gained by a hole in traversing an optical mean free path along the field to the optical-phonon energy, and the ratio of the optical to acoustic path length.

Equations (16) and (17) must be solved numerically. The most economical computational procedure is to eliminate the field term between them and treat T_β as the independent variable. In this way one need solve only a single transcendental equation for T_α. For each pair of temperature values the corresponding field is then obtained from either of the anisotropy balance equations. The values of the various physical parameters we employed in our calculations for a lattice temperature of 77°K are $\epsilon_0=0.037$ eV, $m=0.35m_0$, $l_0 = 783$ Å, $l_a=8300$ Å; the path lengths are based on the low-field mobility studies of Brown and Bray.[21] Although the effective mass does not appear explicitly in (16) and (17), it is necessary in evaluating l_0 and l_a and in calculating transport quantities.

In Fig. 1, heavy-hole energy distributions at 800 and 1350 V/cm computed with the two-temperature model are compared with "exact" energy distributions determined by Budd[10,11] through the more elaborate integral equation method. In the "exact" distributions, the intersection of the Maxwellians is blurred and does not occur precisely at the optical-phonon threshold. Nevertheless, agreement of the two-temperature model results with these distributions is quite good, particularly at high energies. The small discrepancy in T_α can be attributed to our placement of an abrupt intersection at ϵ_0 and neglect of optical-phonon absorption, which Budd did take into account.

Figure 2 displays the field dependence of T_α, T_β, and average temperature $T_{av}[\equiv(2/3k)\langle\epsilon\rangle]$ over a field range $0.47<E<36$ kV/cm. At lower-field strengths, Kurosawa's[9] Monte Carlo calculations indicate that the two-temperature model is not likely to be a good representation. In the lower-field portion of the figure, carriers above the optical-phonon threshold have a lower Maxwellian temperature than those below. This can be attributed to the cooling effect of optical-phonon emission, and is in agreement with previous findings.[9–11] For field strengths in this range, the maximum energy a hole can gain between collisions is much less than ϵ_0. Therefore, only those holes which escape emission of an optical phonon can arrive at high energies. Because the acoustic scattering is relatively weak ($l_a>10l_0$ here) such high-energy holes tend to stream along the field direction, their distribution function taking the form of a narrow spike. Following Shockley's[22] derivation of the field dependence of the ionization rate for streaming carriers, one may conclude that the high-energy holes should have a Maxwellian energy distribution with an average energy proportional to the field. Such a field dependence is displayed by T_β in Fig. 2, which rises nearly linearly with field up to $E\sim4$ kV/cm.

The low-energy temperature T_α attains a broad maximum of value ϵ_0/k in this field range and then begins a gradual descent, intersecting T_β at 5 kV/cm for

[21] D. M. Brown and R. Bray, Phys. Rev. **127**, 1593 (1962).
[22] W. Shockley, Solid State Electron. **2**, 35 (1961).

FIG. 2. Low- and high-energy temperatures (T_α and T_β) versus field. T_{av} is the average temperature of the distribution.

CARRIER TEMPERATURE IN UNITS OF OPTICAL PHONON ENERGY

ELECTRIC FIELD (V/cm)
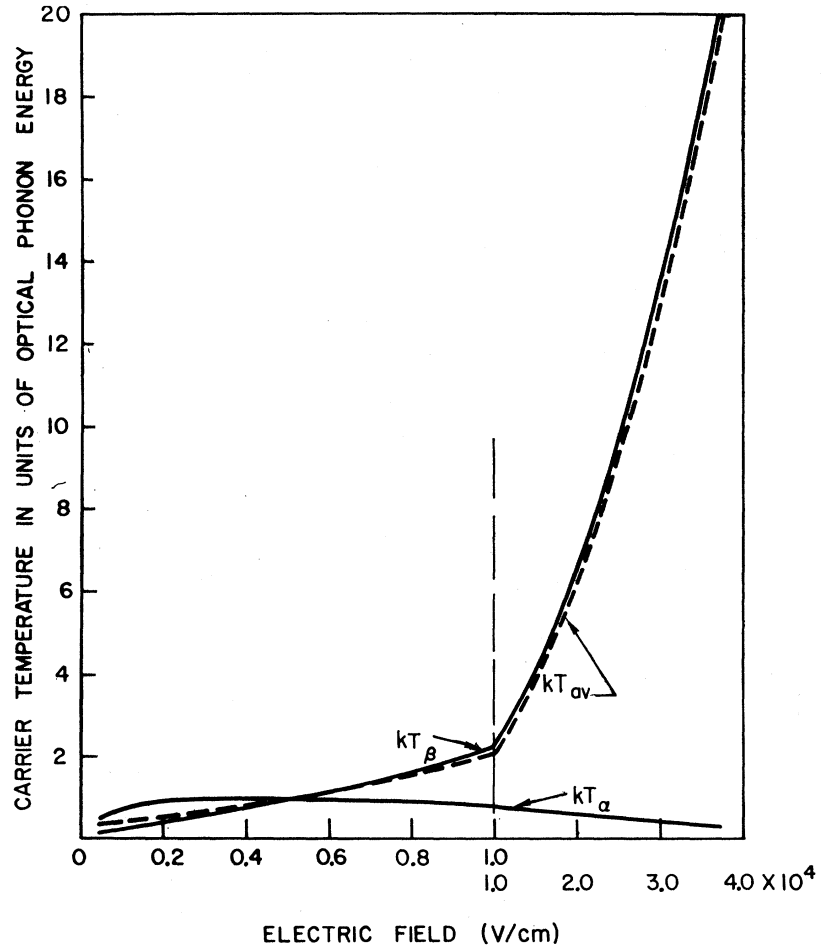
which $Q \approx 1$. A value of Q equal to 1 [see Eq. (18)] denotes that the average energy a hole gains between collisions is about equal to ϵ_0. For fields such that Q exceeds this critical value, it may therefore be anticipated that the distribution function will undergo a qualitative change. When $Q > 1$, holes can remain at high energies after multiple collisions and therefore become more isotropically distributed in momentum space. At the same time, deceleration by the field of holes with negative p_z begins to overcome scattering as the predominant mechanism through which holes arrive at energies below the optical-phonon threshold. As expected, T_β still rises with applied field, but a surprising result is that T_α drops markedly below the value ϵ_0/k. A possible explanation for the low T_α, or, equivalently, a rise in density near the origin, is the following. For $Q \gg 1$, holes starting from relatively large negative p_z can reach the vicinity of the origin within one scattering time. A representative shell of such holes is displaced parallel to the field during this interval with only a reduction in amplitude. Upon arrival at the sphere of radius $p_0 = (2m\epsilon_0)^{1/2}$, inside of which there is relatively little scattering, the large radius shell will first make contact on the p_z axis. The on-axis holes therefore continue into

the sphere unimpeded, while the density of off-axis holes still outside the sphere is diminished further by scattering. The resulting distribution which crosses the plane $p_z = 0$ (for $\epsilon < \epsilon_0$) will then be peaked at the origin. This effect is enhanced because the scattered off-axis holes themselves reenter the distribution in the vicinity of the origin. The actual form of n_0 at low energies is probably quite non-Maxwellian and much smoother at $\epsilon = \epsilon_0$ than the two-temperature model, which makes a Maxwellian best fit, would suggest. However, errors introduced by the inability of the model to exactly represent the low-energy distribution at very high fields should be of small consequence since relatively few carriers will then be found below ϵ_0. This is made evident by the near equality of T_β and T_{av} for $E > 5$ kV/cm. Proceeding toward the right-hand side of the figure, T_β and T_{av} approach the quadratic dependence on field characteristic of the saturated drift velocity region.[20]

IV. MOBILITY

In a manner analogous to the development of the anisotropy balance equations one can derive expressions dependent only on the energy distribution for all trans-
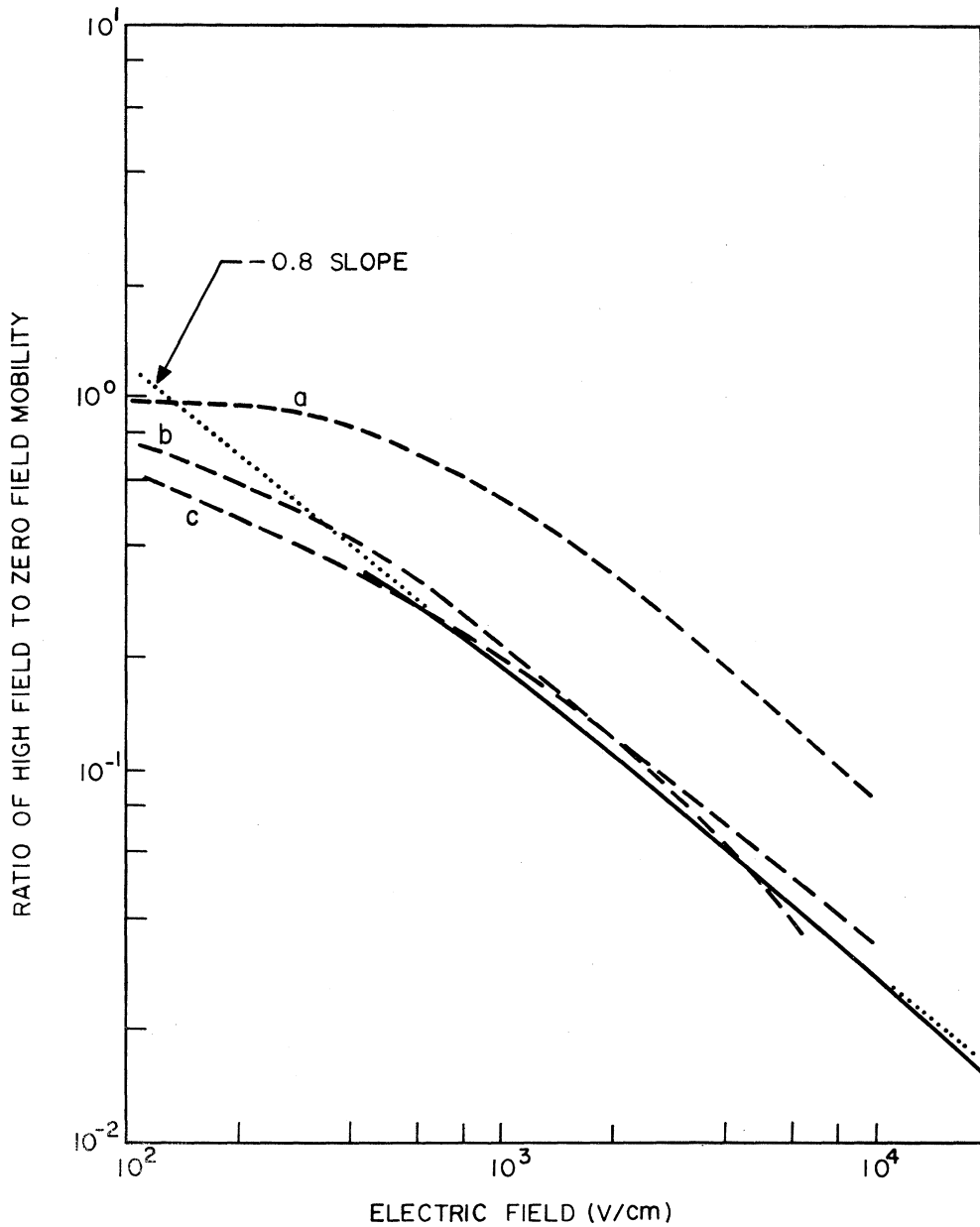
FIG. 3. Theoretical and experimental high-field mobility of p-Ge at 77°K. The solid curve is the two-temperature-model calculation. The dashed curves are experimental results: (a) Ryder (Ref. 23), (b) Mendelson and Bray (Ref. 24), and (c) Zucker (Ref. 25).

port quantities. In the case of the drift velocity this is particularly straightforward. We multiply the first member of (3) by ϵ and perform an energy integration from zero to infinity to obtain

$$\tfrac{1}{3}F\int_0^\infty \frac{d}{d\epsilon}(\epsilon n_1)d\epsilon = (\tfrac{1}{2}m)^{1/2}\int_0^\infty \epsilon^{3/2}\hat{S}n_0 d\epsilon. \quad (20)$$

A partial integration of the left-hand side of (20) yields

$$\tfrac{1}{3}F\int_0^\infty vn_1\epsilon^{1/2}d\epsilon = -(\tfrac{1}{2}m)^{1/2}\int_0^\infty \epsilon^{3/2}\hat{S}n_0 d\epsilon, \quad (21)$$

in which $v=d\epsilon/dp$ is the group velocity. The drift velocity is given by

$$v_d = \tfrac{1}{3}\int_0^\infty vn_1\epsilon^{1/2}d\epsilon \Big/ \int_0^\infty n_0\epsilon^{1/2}d\epsilon, \quad (22)$$

the factor of 3 arising from the Legendre polynomial normalization. Therefore,

$$v_d = -(\tfrac{1}{2}m)^{1/2}\int_0^\infty \epsilon^{3/2}\hat{S}n_0 d\epsilon \Big/ F\int_0^\infty n_0\epsilon^{1/2}d\epsilon. \quad (23)$$
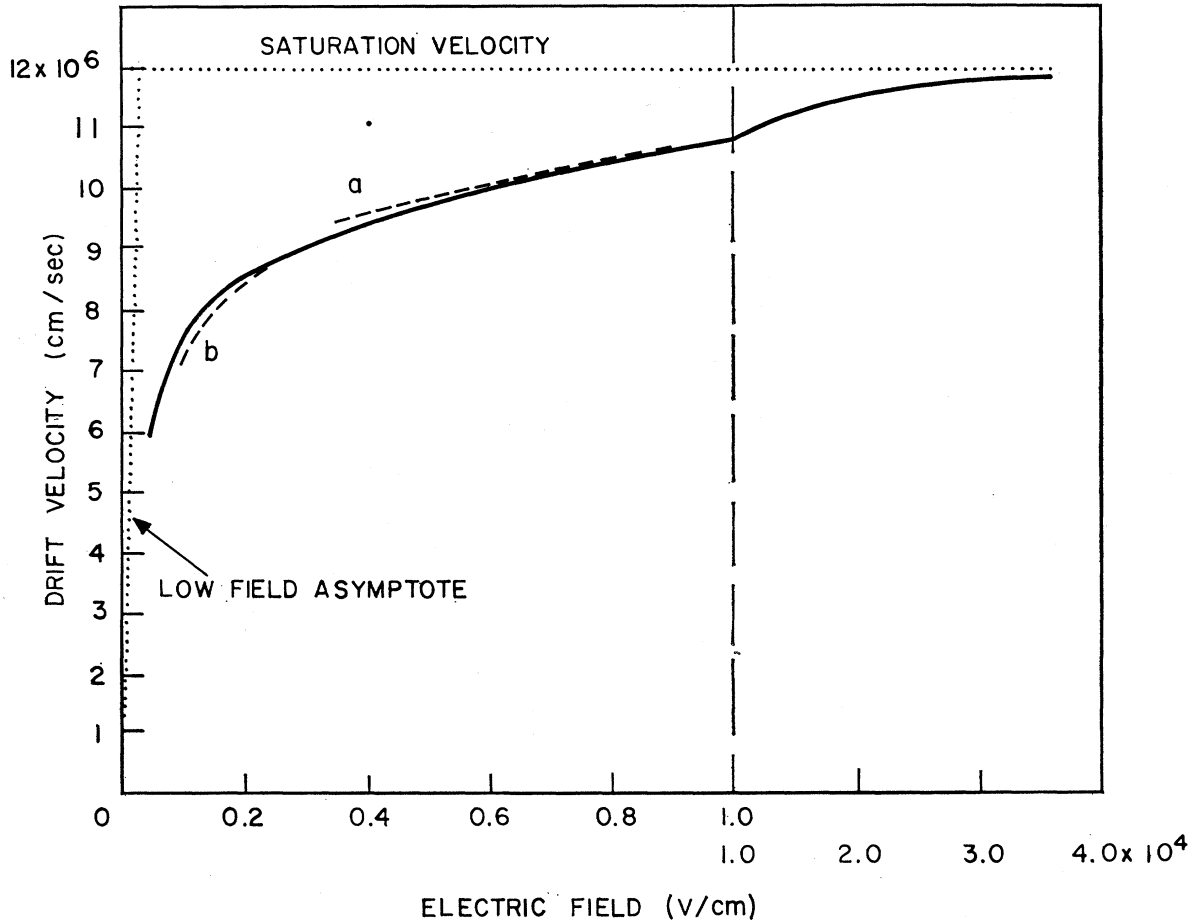
FIG. 4. Velocity-field relation calculated with the two-temperature model (solid curve). The dashed curves are estimated values for three-parameter energy distributions: (a) two-temperature model with variable intersection point and (b) two-temperature energy distribution in displaced coordinate system in momentum space.

Equation (23) is essentially a power balance relation, the numerator on the right-hand side representing the power loss to the scattering system; the presence of this term in (10b) should be noted. The results of computations with this formula, wherein n_0 is represented by the two-temperature model, are given in Figs. 3 and 4.

In Fig. 3 the two-temperature theoretical mobility is compared with experimental data.[23-25] The theoretical curve is normalized to a zero-field heavy-hole mobility of 3.82×10^4 cm²/V sec at 77°K, based on the results of Brown and Bray[21] as were the coupling constants used in determining the distribution function. Thus there are no adjustable parameters. Agreement with the findings of Mendelson and Bray[24] and Zucker[25] is perhaps surprisingly close in view of the fact that the experimental results (conductivity measurements) include the effects of the light holes. The theoretical curve has a slight curvature below 1 kV/cm. Between 1 and 10 kV/cm it

is linear with $\mu \propto E^{-0.8}$, although at somewhat higher fields μ tends toward an E^{-1} dependence. The decade of $E^{-0.8}$ dependence may well be compared with the $E^{-0.8}$ dependence in this field range fitted by Mendelson and Bray, and by Zucker, to their measurements. This initially appeared explicable in terms of emission of acoustic phonons into unpopulated states[26] (zero-point lattice), but the predominant interaction with the optical phonons greatly weakens such an explanation. It is interesting that an equivalent power law arises from the present calculation in which the energy loss is taken to be due to optical-phonon emission and acoustic scattering is assumed to be elastic with equipartition applying.

The heavy-hole velocity-field curve calculated with the two-temperature model for fields up to 37 kV/cm is given in Fig. 4. A fairly pronounced knee in the vicinity of 2 kV/cm and eventual velocity saturation are evident. Also displayed in Fig. 4 are error limits predicted with the error theory of Appendix C. This theory permits an

[23] E. J. Ryder, Phys. Rev. **90**, 766 (1953).
[24] K. S. Mendelson and R. Bray, Proc. Phys. Soc. (London) **B70**, 899 (1957).
[25] J. Zucker, Phys. Chem. Solids **12**, 350 (1960).

[26] B. V. Paranjape, Proc. Phys. Soc. (London) **B70**, 628 (1957).

estimate of the change in a calculated transport quantity that should result from the introduction of an additional parameter into the energy distribution without the necessity for actually evaluating the new distribution. In the case at hand this new distribution would have three parameters (one in addition to the two temperatures) and would satisfy (10c) as well as (10a) and (10b). Curve (a) is the probable velocity-field curve resulting from a parametrization in which the intersection energy of the two Maxwellians is allowed to vary. Curve (b) estimates the velocity-field relation for a model in which there is a two-temperature energy distribution with respect to a variable point in momentum space. Note that this is not similar to a drifted Maxwellian because the distribution need not be isotropic in the new coordinate frame. Numerical difficulties were encountered in these calculations at fields lower than those for which the curves are displayed. Nevertheless, the close agreement of (a), (b), and the solid curve above 4 kV/cm indicates that the drift velocity in this high-field region predicted by the two-temperature model should lie within a few percent of that obtainable by the more exact and cumbersome iterative methods.[9–12] The good agreement between the two-temperature model and (b) down to 1 kV/cm suggests reasonable accuracy at lower fields, which is perhaps better assured by the close correspondence between the two-temperature distribution and that of Budd[10,11] in this field range.

V. DIFFUSION COEFFICIENTS

The diffusion tensor $\mathbf{D}$ is defined by

$$\mathbf{j}_d(r) = -q\nabla \cdot [\mathbf{D}n(\mathbf{r})], \qquad (24)$$

where $\mathbf{j}_d$ is the diffusion current density, n is the carrier density, and both are functions of position $\mathbf{r}$. In order to evaluate $\mathbf{D}$ one must consider the properties of the position-dependent Boltzmann equation

$$\mathbf{F} \cdot \nabla_p f + \frac{1}{m}\mathbf{p} \cdot \nabla f = \int f(\mathbf{p}',\mathbf{r})S(\mathbf{p}',\mathbf{p})d^3p' - \nu f, \quad (25)$$

in which $f(\mathbf{p},\mathbf{r})$ is the position-dependent distribution function. The field force $\mathbf{F}$ may also be nonuniform.

We divide (25) by ν, multiply by $\mathbf{p}$, and integrate the resulting expression over momentum space. For isotropic scattering the collision integral term drops out and we obtain

$$\int \mathbf{p}\nu^{-1}\left(\mathbf{F}\cdot\nabla_p f + \frac{1}{m}\mathbf{p}\cdot\nabla f\right)d^3p = -\int \mathbf{p}fd^3p. \quad (26)$$

Hence the total current density is given by $\mathbf{j} = \mathbf{j}_c + \mathbf{j}_d$,

where

$$\mathbf{j}_c = -\frac{q}{m}\int \mathbf{p}\nu^{-1}\mathbf{F}\cdot\nabla_p f d^3p, \qquad (27a)$$

$$\mathbf{j}_d = -\frac{q}{m^2}\nabla \cdot \int \mathbf{p}\mathbf{p}\nu^{-1}f d^3p. \qquad (27b)$$

Equation (27a) does not involve spatial gradients and is recognized as the conduction current density. Equation (27b) is the diffusion current contribution.

To extract a unique diffusion tensor from a comparison of (24) and (27b) it is necessary to assume that the distribution function is a point function of the field, i.e., we let

$$f(\mathbf{r},\mathbf{p}) = n(\mathbf{r})f_F(\mathbf{p}) \Big/ \int f_F(\mathbf{p})d^3p, \qquad (28)$$

where $n(\mathbf{r})$ is the position-dependent carrier density and $f_F(\mathbf{p})$ is a solution of the spatially homogeneous Boltzmann equation (1) with $\mathbf{F} = \mathbf{F}(\mathbf{r})$. For regions in which the current is strongly space-charge-limited, this approximation is apt to be questionable, and the diffusion tensor will not be a unique function of the field.[2] On the other hand, for small spatial gradients in bulk materials and for current flow in high-field depletion regions it appears well justified.

Introducing (28) into (27b) yields

$$\mathbf{j}_d = -\frac{q}{m^2}\nabla \cdot \left[\left(\int \mathbf{p}\mathbf{p}\nu^{-1}f_F d^3p\right)n(\mathbf{r}) \Big/ \int f_F d^3p\right], \quad (29)$$

from which the diffusion tensor is identified as

$$\mathbf{D} = \frac{1}{m^2}\int \mathbf{p}\mathbf{p}\nu^{-1}f_F d^3p \Big/ \int f_F d^3p. \qquad (30)$$

We now go over to spherical coordinates, expand $f_F(\mathbf{p})$ in Legendre polynomials, and utilize the orthogonality relations for these polynomials. For $\mathbf{F}$ aligned with the z axis, the independent nonvanishing components of $\mathbf{D}$ are found to be

$$D_{\parallel} \equiv D_{zz} = \frac{2}{3}\int_0^\infty \nu^{-1}\epsilon^{3/2}(n_0 + \tfrac{2}{5}n_2)d\epsilon \Big/ m\int_0^\infty \epsilon^{1/2}n_0 d\epsilon, \quad (31a)$$

$$D_{\perp} \equiv D_{xx} = D_{yy} = \frac{2}{3}\int_0^\infty \nu^{-1}\epsilon^{3/2}(n_0 - \tfrac{1}{5}n_2)d\epsilon \Big/ m\int_0^\infty \epsilon^{1/2}n_0 d\epsilon, \quad (31b)$$

which is a generalization to energy-dependent collision frequencies of the diffusion tensor used by Baraff and Buchsbaum.[27] Equations (31a) and (31b) suggest that for anisotropic distributions the longitudinal diffusion will generally exceed the transverse diffusion. In the extreme limit of a spikelike distribution, for which $n_2 = 5n_0$, $D_\perp$ would vanish entirely.

For computational purposes it is convenient to reexpress $D_{||}$ and $D_\perp$ as functions of n_0 alone. Elimination of n_2 from (31a) and (31b) is readily accomplished through algebraic manipulation of the Boltzmann hierarchy (3). Integration of the second member of (3) from zero to ϵ yields

$$n_2 = - \frac{5}{2}\left[\epsilon^{-3/2}\int_0^\epsilon \epsilon^{3/2}\frac{dn_0}{d\epsilon}d\epsilon + \frac{\epsilon^{-3/2}}{F}(\tfrac{1}{2}m)^{1/2}\int_0^\epsilon \epsilon\nu n_1 d\epsilon\right]. \quad (32)$$

Similarly, from the first member of (3) we obtain

$$\epsilon n_1 = \frac{3}{F}(\tfrac{1}{2}m)^{1/2}\int_0^\epsilon \epsilon^{1/2}\hat{S}n_0 d\epsilon. \quad (33)$$

We substitute (33) for ϵn_1 in (32). Hence, we have

$$n_2 = - \frac{5}{2}\left(\epsilon^{-3/2}\int_0^\epsilon \epsilon^{3/2}\frac{dn_0}{d\epsilon}d\epsilon + \frac{3}{2}\frac{m\epsilon^{-3/2}}{F^2}\int_0^\epsilon \nu d\epsilon\int_0^\epsilon \epsilon'^{1/2}\hat{S}n_0'd\epsilon'\right), \quad (34)$$

and after a partial integration of the first term on the right-hand side, we have

$$n_2 = - \frac{5}{2}\left(n_0 - \frac{3}{2}\epsilon^{-3/2}\int_0^\epsilon \epsilon^{1/2}n_0 d\epsilon + \frac{3}{2}\frac{m\epsilon^{-3/2}}{F^2}\int_0^\epsilon \nu d\epsilon\int_0^\epsilon \epsilon'^{1/2}\hat{S}n_0'd\epsilon'\right). \quad (35)$$

Upon inserting (35) into (31a) and (31b), one finds that

$$D_{||} = \left(\frac{1}{m}\int_0^\infty \nu^{-1}d\epsilon\int_0^\epsilon \epsilon'^{1/2}n_0'd\epsilon' - \frac{1}{F^2}\int_0^\infty \nu^{-1}d\epsilon\int_0^\epsilon \nu'd\epsilon'\int_0^{\epsilon'} \epsilon''^{1/2}\hat{S}n_0''d\epsilon''\right) / \int_0^\infty \epsilon^{1/2}n_0 d\epsilon, \quad (36a)$$

[27] G. A. Baraff and S. J. Buchsbaum, Phys. Rev. **130**, 1007 (1963).

$$D_\perp = \left(\frac{1}{m}\int_0^\infty \nu^{-1}\epsilon^{3/2}n_0 d\epsilon - \frac{1}{2m}\int_0^\infty \nu^{-1}d\epsilon\int_0^\epsilon \epsilon'^{1/2}n_0'd\epsilon' + \frac{1}{2F^2}\int_0^\infty \nu^{-1}d\epsilon\int_0^\epsilon \nu'd\epsilon'\int_0^{\epsilon'} \epsilon''^{1/2}\hat{S}n_0''d\epsilon''\right) / \int_0^\infty \epsilon^{1/2}n_0 d\epsilon. \quad (36b)$$

The double and triple integral terms in (36a) and (36b) contain singularities which can be removed by additional partial integrations and the employment of (6a) and (10a). When this is done there results

$$D_{||} = \left(- \frac{1}{m}\int_0^\infty \epsilon^{1/2}\gamma n_0 d\epsilon - \frac{1}{F^2}\int_0^\infty \epsilon^{1/2}\hat{S}n_0 d\epsilon\int_0^\epsilon \nu'\gamma d\epsilon'\right) / \int_0^\infty \epsilon^{1/2}n_0 d\epsilon, \quad (37a)$$

$$D_\perp = \left(\frac{1}{m}\int_0^\infty \nu^{-1}\epsilon^{3/2}n_0 d\epsilon + \frac{1}{2m}\int_0^\infty \epsilon^{1/2}\gamma n_0 d\epsilon + \frac{1}{2F^2}\int_0^\infty \epsilon^{1/2}\hat{S}n_0 d\epsilon\int_0^\epsilon \nu'\gamma'd\epsilon'\right) / \int_0^\infty \epsilon^{1/2}n_0 d\epsilon, \quad (37b)$$

where

$$\gamma \equiv \int_0^\epsilon \nu^{-1}d\epsilon.$$

Figure 5 shows the field dependence of the heavy-hole diffusion coefficients computed from (37a) and (37b) with the two-temperature model. The elongation of the distribution function along the field results in $D_{||} > D_\perp$, but the anisotropy never gets very large. Perhaps more significant is that over the range of fields covered neither coefficient departs greatly from the zero-field value, in qualitative agreement with noise temperature measurements that have been carried out on n-Ge.[6] It may be inferred from Fig. 5 that the strongest field dependence must be that of $D_{||}$ in the warm-carrier region not considered. The longitudinal diffusion of minority holes in n-Ge at 77°K has been measured for the field range $10 < E < 500$ V/cm by Okamoto et al.[7] Their experimental data shows a rapid rise in $D_{||}$, but to much higher values ($D_{||} \sim 5 \times 10^4$ cm²/sec at their field maximum of 500 V/cm) than one would expect from either a hot-carrier Einstein relation[28] or the present theory.

[28] J. Zucker and E. M. Conwell, in *Proceedings of the International Conference on the Physics of Semiconductions, Exeter, 1962*, edited by A. C. Strickland (The Institute of Physics and the Physical Society, London, 1962), p. 851.
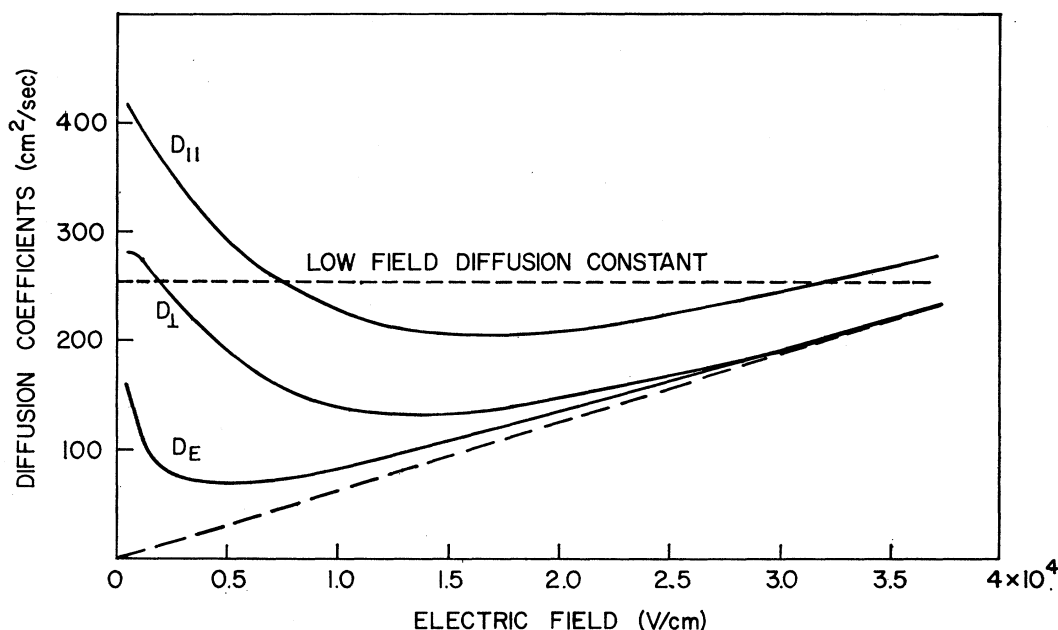
FIG. 5. Field dependence of the diffusion coefficients: $D_{||}$, parallel to field; $D_{\perp}$, normal to field. $D_E = \mu k T_{av}/q$ is the Einstein diffusion coefficient. The dashed line passing through the origin is the high-field asymptote. The horizontal dashed line is the zero-field diffusion constant.

Although some enhancement of diffusion might be attributed to the light holes, it appears possible that damping due to boundary effects is responsible for the greatest increase.

At the highest fields shown, both $D_{||}$ and $D_{\perp}$ approach a linear field dependence. This result is expected in the saturated drift velocity regime where the distribution function becomes an isotropic Maxwellian[20] for which the Einstein relation is valid, the mobility decreases inversely with the field, and the carrier temperature increases with the square of the field. The curve labeled D_E is a hot-carrier Einstein relation which uses the average carrier temperature and total mobility computed with the two-temperature model. At low and intermediate fields it somewhat underestimates both diffusion coefficients, but coalesces with $D_{\perp}$ before the velocity saturation region is reached.

Note added in proof. High-field diffusion coefficients for silicon at room temperature, indicating a drop below the low field value, have recently been measured. See T. W. Sigmon and J. F. Gibbons, Appl. Phys. Letters **15**, 320 (1969); D. J. Bartelink and G. Persky, *ibid.* (to be published).

ACKNOWLEDGMENTS

APPENDIX A: INTERPRETATION OF (6b) FOR $l=1, 2$

For $l=1$, Eq. (6b) takes the form

$$F \int_0^\infty \epsilon^{1/2} n_0 d\epsilon = \tfrac{2}{3}(\tfrac{1}{2}m)^{1/2} \int_0^\infty \epsilon \nu n_1 d\epsilon$$

$$= \tfrac{1}{3}m \int_0^\infty v\epsilon^{1/2}\nu n_1 d\epsilon. \qquad (A1)$$

Letting $\langle \ \rangle$ denote expectation value, (A1) becomes

$$F\langle f \rangle = m\langle v_z \nu f \rangle, \qquad (A2)$$

where we have utilized the orthogonality and normalization properties of the Legendre polynomials. Equation (A2) expresses the equality between the field force density and time rate of momentum density loss to the scattering system.

When $l=2$, Eq. (6b) becomes

$$\tfrac{1}{3}F \int_0^\infty \epsilon n_1 d\epsilon = \tfrac{1}{5}(\tfrac{1}{2}m)^{1/2} \int_0^\infty \epsilon^{3/2} \nu n_2 d\epsilon \qquad (A3)$$

or

$$\tfrac{1}{3}F \int_0^\infty v\epsilon^{1/2} n_1 d\epsilon = \tfrac{1}{10}m \int_0^\infty v^2 \epsilon^{1/2} \nu n_2 d\epsilon. \qquad (A4)$$

Introducing the orthogonality relations yields

$$F\langle v_z f \rangle = \tfrac{1}{4}m\langle (3v_z{}^2 - v^2)\nu f \rangle. \qquad (A5)$$

The left-hand side is the power input density from the field. The right-hand side (the presence of an n_2 component) shows that anisotropy must result from this power input.

The usual power balance relation that can easily be derived directly from the Boltzmann equation (1) is

$$F\langle v_z f\rangle = -\langle \epsilon(\partial f/\partial t)_{\text{col}}\rangle, \qquad (A6)$$

where $(\partial f/\partial t)_{\text{col}}$ is the collision derivative. Equation (A5) is not identical to this relation. Together, (A5) and (A6) imply that

$$\langle(3v_z{}^2-v^2)\nu f\rangle = -2\langle v^2(\partial f/\partial t)_{\text{col}}\rangle \qquad (A7)$$

when the scattering is isotropic and the carrier heating is due to an applied field.

APPENDIX B: ANISOTROPY BALANCE EQUATIONS FOR NONPARABOLIC BANDS AND ANISOTROPIC SCATTERING

The Boltzmann equation (1) can be written in the form

$$[(\mathbf{F}\cdot\nabla_p-\hat{\sigma})f=0, \qquad (B1)$$

where

$$\hat{\sigma}f\equiv\int f(\mathbf{p}')S(\mathbf{p}',\mathbf{p})d^3p'-\nu(\mathbf{p})f(\mathbf{p}). \qquad (B2)$$

We premultiply (B1) by an arbitrary function $G(\mathbf{p})$ and integrate over momentum space. Clearly,

$$\int G(\mathbf{F}\cdot\nabla_p-\hat{\sigma})fd^3p=0. \qquad (B3)$$

An adjoint scattering operator $\hat{\sigma}^\dagger$ may be defined such that

$$\hat{\sigma}^\dagger G=\int G(\mathbf{p}')S(\mathbf{p},\mathbf{p}')d^3p'-\nu(\mathbf{p})G(\mathbf{p}). \qquad (B4)$$

It follows that

$$\int G\hat{\sigma}fd^3p=\int f\hat{\sigma}^\dagger Gd^3p. \qquad (B5)$$

By performing a partial integration of the field term and invoking (B5), (B3) can be recast as

$$\int f(\mathbf{F}\cdot\nabla_p+\hat{\sigma}^\dagger)Gd^3p=0. \qquad (B6)$$

We now impose on G the condition

$$\int_0^\pi P_l(\cos\theta)(\mathbf{F}\cdot\nabla_p+\hat{\sigma}^\dagger)G(\mathbf{p})\sin\theta d\theta=0, \quad l\geq 1 \quad (B7)$$

and define a new function $h(p)$ by

$$\int_0^\pi (\mathbf{F}\cdot\nabla_p+\hat{\sigma}^\dagger)G(\mathbf{p})\sin\theta d\theta\equiv 2h(p)\neq 0. \qquad (B8)$$

Then (B6) reduces to

$$\int_0^\infty p^2 n_0(p)h(p)dp=0, \qquad (B9)$$

where $n_0(p)$ is the isotropic component of the distribution function. The exact $n_0(p)$ must satisfy (B9) for all $h(p)$ defined by (B8), wherein $G(p)$ satisfies (B7). Equation (B9) will yield a distinct anisotropy balance equation for each independent function G that satisfies (B7) and results in a nonvanishing h.

Explicit solutions for G are obtainable if the scattering operator $\hat{\sigma}$, and hence $\hat{\sigma}^\dagger$, are diagonal in the Legendre polynomial representation. It is a well-known result[29] that the diagonality requirement is met when the band has rotational symmetry about the field direction and the scattering probability has the form $S(\mathbf{p}',\mathbf{p})=S(|\mathbf{p}'-\mathbf{p}|)$.

This property is most easily exploited if we make the expansion

$$G(\mathbf{p})=\sum_{\nu=0}^\infty g_\nu(p)P_\nu(\cos\theta). \qquad (B10)$$

It then follows that

$$\hat{\sigma}^\dagger G=\sum_{\nu=0}^\infty \hat{s}_\nu{}^\dagger g_\nu(p)P_\nu(\cos\theta), \qquad (B11)$$

and (B7) and (B8) can be expressed in component form as

$$F\left(\frac{l+1}{2l+3}\frac{d}{dp}(p^{l+2}g_{l+1})+\frac{l}{2l-1}p^{2l+1}\frac{d}{dp}(p^{1-l}g_{l-1})\right)$$
$$+p^{l+2}\hat{s}_l{}^\dagger g_l=0, \quad l\geq 1 \quad (B12)$$

$$\tfrac{1}{3}F(d/dp)(p^2 g_1)+p^2 s_0{}^\dagger g_0=p^2 h(p). \qquad (B13)$$

To utilize (B12) and (B13), one first finds a G satisfying the coupled set of equations (B12), and then inserts the resulting g_1 and g_0 into (B13) to produce an h. An anisotropy balance equation is obtained upon substitution of h into (B9). Functions G which satisfy (B12) exactly can be found by terminating (B10) after a finite number of terms. Successive functions G generate consecutive members of the set of anisotropy balance equations. We shall derive the first few.

Let $G(\mathbf{p})=g_0(p)$. Then for $l=1$, (B12) reduces to

$$dg_0/dp=0, \qquad (B14)$$

[29] B. Davison, *Neutron Transport Theory* (Oxford University Press, New York, 1957), Sec. 17.1.

with the solution $g_0 =$ const. For convenience we take this constant to be unity. Equation (B13) then yields

$$h(p) = (\hat{s}_0{}^\dagger 1). \tag{B15}$$

Accordingly, from (B9) we obtain

$$\int_0^\infty p^2 n_0(\hat{s}_0{}^\dagger 1)dp = 0 \tag{B16}$$

or

$$\int_0^\infty p^2 \hat{s}_0 n_0 dp = 0. \tag{B17}$$

Equation (B17) is the continuity equation and is equivalent to (6a).

We now let $G(\mathbf{p}) = g_0(p) + g_1(p) \cos\theta$. Then from (B12), with $l=2$, we have

$$(d/dp)(p^{-1}g_1) = 0 \tag{B18}$$

and hence

$$g_1 = p. \tag{B19}$$

Inserting (B19) into the $l=1$ member of (B12) yields

$$F(dg_0/dp) + (\hat{s}_1{}^\dagger p) = 0 \tag{B20}$$

which has the solution

$$g_0 = -\frac{1}{F}\int_0^p (\hat{s}_1{}^\dagger p)dp. \tag{B21}$$

Substitution of (B19) and (B21) into (B13) results in

$$\tfrac{1}{3}F\frac{d}{dp}(p^3) - \frac{p^2}{F}\left(\hat{s}_0{}^\dagger \int_0^p (\hat{s}_1{}^\dagger p)dp\right) = p^2 h. \tag{B22}$$

Thus,

$$h = F - \frac{1}{F}\left(\hat{s}_0{}^\dagger \int_0^p (\hat{s}_1{}^\dagger p)dp\right), \tag{B23}$$

and (B9) becomes

$$F\int_0^\infty p^2 n_0 dp$$
$$-\frac{1}{F}\int_0^\infty p^2 n_0\left(\hat{s}_0{}^\dagger \int_0^p (\hat{s}_1{}^\dagger p')dp'\right)dp = 0 \tag{B24}$$

or

$$F^2\int_0^\infty p^2 n_0 dp - \int_0^\infty p^2(\hat{s}_0 n_0)\int_0^p (\hat{s}_1{}^\dagger p')dp'dp = 0. \tag{B25}$$

Equation (B25) constitutes the generalization of (10a) to anisotropic scattering and nonparabolic bands. It reduces to (10a) upon setting $p = (2m\epsilon)^{1/2}$, $\hat{s}_1{}^\dagger = -\nu$ and $\hat{s}_0 = \hat{S}$.

The generalization of (10b) may be generated in similar fashion. In this case we let $G = g_0 + g_1 \cos\theta + g_2 \times P_2(\cos\theta)$, and we solve for g_2 with the $l=3$ member of

(B12), obtaining $g_2 = p^2$. Then, proceeding as before, we find g_1, g_0, and h. The resultant anisotropy balance equation is

$$F^2\int_0^\infty p^4(\hat{s}_0 + \tfrac{1}{2}\hat{s}_2)n_0 dp$$

$$+\tfrac{3}{2}F^2\int_0^\infty p^2 n_0\int_0^p \frac{1}{p'}(\hat{s}_2{}^\dagger p'^2)dp'dp - \tfrac{3}{2}\int_0^\infty p^2(\hat{s}_0 n_0)$$

$$\times \int_0^p \left(\hat{s}_1{}^\dagger p'\int_0^{p'}\frac{1}{p''}(\hat{s}_2{}^\dagger p''^2)dp''\right)dp'dp = 0. \tag{B26}$$

Equations (B25) and (B26) have been employed by the authors in a calculation of the high-field electron mobility in InSb.[30]

APPENDIX C: ERROR-ESTIMATE THEORY

In this appendix we develop a method for estimating small changes in a calculated transport quantity resulting from the introduction of an additional *infinitesimal* parametrization of a parametrized energy distribution. The technique permits assessment of the sensitivity of transport calculations to such changes in the parametrization without the necessity for actual solution of additional anisotropy balance equations. Although carried out for a parabolic band, it may be readily generalized.

Consider an energy distribution $n_0(\epsilon; \alpha_1, \ldots, \alpha_m)$ found by solving the first m members of (10) for the parameters $\alpha_1, \ldots, \alpha_m$. These anisotropy balance equations may be expressed symbolically as

$$\int_0^\infty \hat{D}_i n_0(\epsilon; \alpha_1, \ldots, \alpha_m)d\epsilon = D_i = 0, \quad i = 1, \ldots, m. \tag{C1}$$

The $(m+1)$th equation is not satisfied:

$$\int_0^\infty \hat{D}_{m+1} n_0(\epsilon; \alpha_1, \ldots, \alpha_m)d\epsilon = D_{m+1} \neq 0. \tag{C2}$$

We now introduce into n_0 an additional parameter α_{m+1} in such a way that for $\alpha_{m+1} = 0$ the new distribution is identical to the original one, i.e.,

$$n_0(\epsilon; \alpha_1, \ldots, \alpha_{m+1})|_{\alpha_{m+1}=0} = n_0(\epsilon; \alpha_1, \ldots, \alpha_m). \tag{C3}$$

With $\alpha_{m+1} = 0$ the new distribution still satisfies the set of equations (C1), but not (C2). If we let α_{m+1} depart from zero in order to satisfy (C2), this must be done in a way such that (C1) remains satisfied, i.e., (C1) provides a system of constraints relating variations in $\alpha_1, \ldots, \alpha_m$ to any variation imposed upon α_{m+1}. Thus, to

[30] G. Persky and D. J. Bartelink, Bull. Am. Phys. Soc. 14, 748 (1969); IBM J. Res. Dev. 13, 607 (1969).

first order we have

$$0 = \delta D_i = \int_0^\infty \hat{D}_i \sum_{j=1}^{m+1} \delta\alpha_j \frac{\partial}{\partial\alpha_j} n_0(\epsilon;\alpha_1,\ldots,\alpha_{m+1})d\epsilon \Big|_{\alpha_{m+1}=0},$$
$$i=1,\ldots,m \quad (C4)$$

which results in the system of equations

$$-D_{i,m+1}\delta\alpha_{m+1} = \sum_{j=1}^{m} D_{ij}\delta\alpha_j, \quad i=1,\ldots,m \quad (C5)$$

where

$$D_{ij} \equiv \int_0^\infty \hat{D}_i \frac{\partial}{\partial\alpha_j} n_0(\epsilon;\alpha_1,\ldots,\alpha_m)d\epsilon, \quad j=1,\ldots,m \quad (C6)$$

and

$$D_{i,m+1} \equiv \int_0^\infty \hat{D}_i \frac{\partial}{\partial\alpha_{m+1}} n_0(\epsilon;\alpha_1,\ldots,\alpha_{m+1})d\epsilon \Big|_{\alpha_{m+1}=0}. \quad (C7)$$

Given $\delta\alpha_{m+1}$, the system (C5) provides m equations for the $\delta\alpha_j$ ($j=1,\ldots,m$) and may be inverted to solve for these variations. We shall suppose this to have been done. Then

$$\delta\alpha_j = \Gamma_j \delta\alpha_{m+1}, \quad (C8)$$

where

$$\Gamma_j = -\sum_{k=1}^{m} C_{jk}D_{k,m+1}, \quad \sum_{j=1}^{m} C_{ij}D_{jk} = \delta_{ik}. \quad (C9)$$

The variation of D_{m+1} is given by

$$\delta D_{m+1} = \int_0^\infty \hat{D}_{m+1} \sum_{j=1}^{m+1} \delta\alpha_j$$
$$\times \frac{\partial}{\partial\alpha_j} n_0(\epsilon;\alpha_1,\ldots,\alpha_{m+1})d\epsilon \Big|_{\alpha_{m+1}=0}, \quad (C10)$$

which, upon invoking (C8) and the definitions (C6) and (C7), becomes

$$\delta D_{m+1} = \delta\alpha_{m+1} \sum_{j=1}^{m+1} \Gamma_j D_{m+1,j}. \quad (C11)$$

For convenience we have defined

$$\Gamma_{m+1} = 1. \quad (C12)$$

We now examine the variation of a macroscopic transport quantity $\bar{A}$, where

$$\bar{A} = \int_0^\infty \hat{a} n_0 d\epsilon \Big/ \int_0^\infty \epsilon^{1/2} n_0 d\epsilon. \quad (C13)$$

For generality $\hat{a}$ may involve linear operations on $n_0(\epsilon)$ other than simple multiplication. The variation of $\bar{A}$ produced by the parameter variation is given by

$$\delta\bar{A} = \left(\int_0^\infty \epsilon^{1/2} n_0 d\epsilon \int_0^\infty \hat{a} \sum_{j=1}^{m+1} \delta\alpha_j \frac{\partial}{\partial\alpha_j} n_0(\epsilon;\alpha_1,\ldots,\alpha_{m+1})d\epsilon \Big|_{\alpha_{m+1}=0} \right.$$
$$\left. - \int_0^\infty \hat{a} n_0 d\epsilon \int_0^\infty \epsilon^{1/2} \sum_{j=1}^{m+1} \delta\alpha_j \frac{\partial}{\partial\alpha_j} n_0(\epsilon;\alpha_1,\ldots,\alpha_{m+1})d\epsilon \Big|_{\alpha_{m+1}=0} \right) \Big/ \left(\int_0^\infty \epsilon^{1/2} n_0 d\epsilon \right)^2. \quad (C14)$$

Upon introducing (C8) and (C12), (C14) becomes

$$\delta\bar{A} = \delta\alpha_{m+1} \sum_{j=1}^{m+1} \Gamma_j \left(\int_0^\infty \epsilon^{1/2} n_0 d\epsilon \int_0^\infty \hat{a} \frac{\partial}{\partial\alpha_j} n_0(\epsilon;\alpha_1,\ldots,\alpha_{m+1})d\epsilon \Big|_{\alpha_{m+1}=0} \right.$$
$$\left. - \int_0^\infty \hat{a} n_0 d\epsilon \int_0^\infty \epsilon^{1/2} \frac{\partial}{\partial\alpha_j} n_0(\epsilon;\alpha_1,\ldots,\alpha_{m+1})d\epsilon \Big|_{\alpha_{m+1}=0} \right) \Big/ \left(\int_0^\infty \epsilon^{1/2} n_0 d\epsilon \right)^2. \quad (C15)$$

Finally, upon dividing (C15) by (C11), we obtain

$$\frac{\delta\bar{A}}{\delta D_{m+1}} = \sum_{j=1}^{m+1} \Gamma_j \left(\int_0^\infty \epsilon^{1/2} n_0 d\epsilon \int_0^\infty \hat{a} \frac{\partial}{\partial\alpha_j} n_0(\epsilon;\alpha_1,\ldots,\alpha_{m+1})d\epsilon \Big|_{\alpha_{m+1}=0} \right.$$
$$\left. - \int_0^\infty \hat{a} n_0 d\epsilon \int_0^\infty \epsilon^{1/2} \frac{\partial}{\partial\alpha_j} n_0(\epsilon;\alpha_1,\ldots,\alpha_{m+1})d\epsilon \Big|_{\alpha_{m+1}=0} \right) \Big/ \sum_{j=1}^{m+1} \Gamma_j D_{m+1,j} \left(\int_0^\infty \epsilon^{1/2} n_0 d\epsilon \right)^2, \quad (C16)$$

which represents the infinitesmal variation of $\bar{A}$ with D_{m+1}. Thus we may take

$$\Delta\bar{A} \equiv -(\delta\bar{A}/\delta D_{m+1})D_{m+1} \qquad \text{(C17)}$$

as a first-order estimate of the change that would be introduced into the calculated value of $\bar{A}$ by adding another parameter to the energy distribution and satisfying the expanded set of anisotropy balance equations. It should be noted that $\Delta\bar{A}$ is not unique, but depends upon the particular additional parametrization chosen. A small value of $\Delta\bar{A}$ implies that either the transport quantity $\bar{A}$ is not sensitive to the particular additional parametrization $(\delta\bar{A}/\delta D_{m+1} \to 0)$ or the anisotropy balance equation $D_{m+1} = 0$ is well satisfied for small α_{m+1}. To establish the quality of the initial m-parameter model, in principle one would have to perform the error test with all possible $m+1$ parametrizations, obtaining small $\Delta\bar{A}$ for each. In practice, a priori knowledge of reasonable forms for the energy distribution will allow this test to be carried out with a particular finite set. An example, wherein $\bar{A}$ is the drift velocity, is given in Sec. IV.

Lifetimes of Bound Excitons in CdS

C. H. HENRY AND K. NASSAU

Bell Telephone Laboratories, Murray Hill, New Jersey 07974

(Received 23 September 1969)

Weakly bound excitons in CdS have giant oscillator strengths which lead to exceedingly fast radiative lifetimes. We have been able to measure the lifetime of the I_2 line, an exciton bound to a neutral donor, and the lifetime of the I_1 line, an exciton bound to a neutral acceptor. We find $\tau_{I_2} = 0.5 \pm 0.1$ nsec and $\tau_{I_1} = 1.03 \pm 0.1$ nsec. The measurements were made at 1.6°K. The lifetimes are measured by exciting the luminescence with an argon laser modulated at 100 Mc/sec, and measuring the time delay of the luminescence with a 100-Mc/sec phase-sensitive detector. Previous calculations by Rashba and Guygenishvili predicted radiative lifetimes which were an order of magnitude shorter than our measured values. They used an incorrect value for the exciton mass. When corrected, their theory gives $\tau_{I_2} = 0.56$ nsec and $\tau_{I_1} = 1.86$ nsec, in reasonably good agreement with our measurements. Thomas and Hopfield measured the absorption oscillator strength of the I_2 line. Their measurements predict a radiative lifetime for the I_2 line of 0.4 ± 0.1 nsec. This is very close to our measured value and shows that the I_2 line decays radiatively. We conclude that the nonradiative Auger effect is negligible for the I_2 line and either negligible or small for the I_1 line. We also calculate the lifetime for donor-acceptor pair recombination to be 2.2 nsec as the pair separation goes to zero. This agrees with Colbow's experimental value of 2.5 ± 1 nsec. Using the same method, we calculate the lifetime of the Te isoelectronic trap to be 27 nsec. This agrees poorly with Cuthbert and Thomas's measured value of 300 nsec.

I. INTRODUCTION

THE edge emission in CdS, at helium temperature, consists primarily of donor-acceptor pair recombination in the green and the decay of excitons bound to neutral donors and acceptors in the blue. The decay of the bound excitons consists of sharp no-phonon lines followed by much weaker phonon sidebands. These transitions are shown in Fig. 1. The I_2 line is the decay of an exciton bound to a neutral donor and the I_1 line is the decay of an exciton bound to a neutral acceptor. In this paper, we report the measurement of the lifetimes of the I_1 and I_2 lines in CdS at 1.6°K.

The I_1 and I_2 lines were analyzed by Thomas and Hopfield[1] in 1962. That same year, Rashba and Gurgenishvili[2] (hereafter referred to as RG) showed that in a direct band gap semiconductor, such as CdS, the oscillator strength for radiative decay of a weakly bound exciton could be simply calculated in terms of the binding energy of the bound exciton, the exciton mass, and the oscillator strength per molecule of the free exciton. They pointed out that excitons, weakly bound to impurities, have giant oscillator strengths that are many orders of magnitude larger than the oscillator strength per molecule of the free exciton. Using values which they thought appropriate for bound excitons (the I_2 lines) in CdS, they concluded that the oscillator strength was roughly a factor of 4×10^4 greater than the oscillator strength of the free exciton per molecule in CdS, i.e., the oscillator strength was about 80. The ideas of RG were qualitatively verified at the time of publication, because they explained why impurity absorption just below the free exciton was so strong in undoped relatively pure semiconductors such as CdS. From the oscillator strength, one can predict both the absorption strength and the radiative lifetime of the bound exciton. Their value of the oscillator strength would give a radiative lifetime of about 0.044 nsec.

[1] D. G. Thomas and J. J. Hopfield, Phys. Rev. **128**, 2135 (1962).

[2] E. I. Rashba and G. E. Gurgenishvili, Fiz. Tverd. Tela **4**, 1029 (1962) [English transl.: Soviet Phys.—Solid State **4**, 759 (1962)] (referred to as RG in this paper).